Patient-derived organoids for cystic fibrosis drug discovery ofbiological validity and screening scalability

Umayyah Osman [1*]

Abstract

Cystic fibrosis remains a monogenic disease with a stubbornly heterogeneous therapeutic landscape. Small-molecule CFTR modulators now benefit most people carrying F508del, yet roughly one in ten patients — those with premature termination codons, ultra-rare missense alleles, or deep intronic splicing defects — derive little or no benefit, and even genotypically identical individuals respond unevenly. Patient-derived three-dimensional organoids have emerged as the preclinical system best positioned to close that gap. This review evaluates how far organoid-based high-throughput screening has actually come, separating what the evidence supports from what remains aspirational. We examine four questions in turn: whether organoids are biologically valid surrogates for the patient; whether the functional assays built on them measure what they claim to measure; whether those assays genuinely scale; and whether the platform can validate the nucleic acid and gene editing therapies now entering development. The forskolin-induced swelling assay anchors the field, and its concordance with sweat chloride, ppFEV1, and nasal potential difference is strong enough to have guided real prescribing decisions through initiatives such as HIT-CF. Miniaturization into 384-well formats, robotic liquid handling, and deep-learning image analysis — OrgaQuant, DETECTOR, OrgaSegment — have converted a laborious bench assay into a screening platform with acceptable statistical power. Opened-organoid monolayers resolve the geometric problem of an enclosed apical membrane, extending screening to ENaC, TMEM16A, and SLC6A14. Substantial obstacles persist, however: matrix variability, tissue-specific regulatory differences, cost, and the absence of a regulatory framework qualifying organoid response as a surrogate endpoint. We argue these are tractable engineering and governance problems rather than biological ones.

Keywords

cystic fibrosis; CFTR; patient-derived organoids; forskolin-induced swelling; high-throughput screening; theratyping; prime editing; deep learning

1. Introduction

Cystic fibrosis (CF) is an autosomal recessive, multisystem disorder arising from loss-of-function mutations in the gene encoding the cystic fibrosis transmembrane conductance regulator (Cutting, 2015). CFTR itself is a cyclic adenosine monophosphate (cAMP)-dependent, phosphorylation-activated anion channel; its job is to move chloride and bicarbonate across epithelial

Significance | Patient-derived organoid screening converts cystic fibrosis genotype into actionable, individualized treatment decisions for rare variants that modulator therapy cannot otherwise reach.

Correspondence.

Umayyah Osman, Quest International University, Faculty of Medicine, Malaysia. E-mail: umayyahedu@gmail.com.

Editor Md Fakruddin, Ph.D. And accepted by the Editorial Board Oct 31, 2026 (received for review Sep 4, 2026)

Author Affiliation:

[1] Quest International University, Faculty of Medicine, Malaysia.

Please cite this article as: Osman, U. (2026). "Patient-derived organoids for cystic fibrosis drug discovery of biological validity and screening scalability", Integrative Biomedical Research, 10(2), 1-23, 10961

3068-6326/© 2026 (Integrative Biomedical Research), a publication of Eman Research, USA.
This is an open access article under the CC BY-NC-ND license.
(http://creativecommons.org/licenses/by-nc-nd/4.0/)
(https://publishing.emanresearch.org)

membranes, and through that movement to govern surface hydration, luminal pH, and fluid homeostasis (Ratjen et al., 2015). When the channel fails, the downstream consequences follow a grimly predictable sequence — airway surface liquid depletion, viscous mucus accumulation, impaired mucociliary clearance, chronic bacterial colonization, and eventually progressive respiratory failure, which remains the dominant cause of death (Ratjen et al., 2015). More than 2,000 variants have been catalogued at the CFTR locus, conventionally sorted into functional classes according to whether the primary defect lies in synthesis, trafficking, gating, conductance, or splicing (Cutting, 2015).

The arrival of small-molecule CFTR modulators altered that trajectory considerably. Correctors such as lumacaftor, tezacaftor, and elexacaftor, paired with the potentiator ivacaftor, have transformed clinical management for patients carrying common class II missense variants, F508del above all (Keating et al., 2018). The qualification matters, though. Approximately 10% of the CF population carries rare or ultra-rare alleles — premature termination codon (PTC) nonsense mutations such as W1282X, G542X, R553X, and S308X among them — that never produce full-length CFTR protein and therefore present no substrate for a corrector to rescue (Berical et al., 2022; Tsai et al., 2025). Nor is the picture uniform even within a single genotype. Patients homozygous for F508del display a wide spread of clinical severity and modulator responsiveness, differences attributable to secondary genetic modifiers and epigenetic variation rather than to the causal allele itself (Berkers et al., 2019; Conti et al., 2022). What follows from this is a fairly specific need: physiologically faithful human cell models capable of guiding individualized prescribing, supporting theratyping, and sustaining high-throughput screening (HTS) of small molecules, nucleic acid therapeutics, and gene editing reagents.

For much of the field's history, that need went unmet. Preclinical CF drug discovery rested on two-dimensional immortalized cell lines or on primary human bronchial epithelial cultures grown at an air–liquid interface (ALI) (Pacheco et al., 2022). ALI cultures remain valuable — short-circuit current (Isc) measurement in Ussing chambers is still the gold standard for quantifying transepithelial ion transport, and nothing has displaced it (Pranke et al., 2017). But finite expansion capacity, dependence on invasively obtained explant tissue, and an intrinsically low ceiling on throughput make these systems poorly suited to screening compound libraries at scale (Amatngalim et al., 2022; Conti et al., 2022). Three-dimensional organoids offered a way around each constraint. Derived from adult stem cells (ASCs) harvested through minimally invasive rectal biopsy or nasal brushing, or generated from patient-specific induced pluripotent stem cells (iPSCs), these self-renewing epithelial structures reproduce native tissue architecture and cellular diversity while remaining genetically the patient's own (Sato et al., 2009; Dekkers et al., 2013).

The assay that made organoids useful rather than merely interesting is forskolin-induced swelling (FIS), introduced by Dekkers et al. (2013). Forskolin activates adenylyl cyclase, raising intracellular cAMP; CFTR opens; chloride and water flux into the enclosed lumen; the organoid visibly expands, and that expansion can be quantified (Boj et al., 2017). The elegance of the readout lies in its dependency: in intestinal organoids, swelling is strictly CFTR-dependent. Organoids from healthy donors swell briskly, CF-derived organoids barely at all, and the defect is reversed by effective modulators or by genetic correction (Dekkers et al., 2013; Geurts et al., 2020). Steady-state lumen area (SLA) supplies a complementary, static measure of resting luminal dimension, useful where baseline fluid retention confounds the dynamic readout (Xia et al., 2021).

Why should an intestinal structure predict a pulmonary outcome? The answer rests on what organoids preserve. Unlike heterologous overexpression systems, they retain the donor's (epi)genetic background, endogenous regulatory elements, and native splicing machinery, so CFTR is expressed at physiological levels under physiological control (Pacheco et al., 2022). Empirically, the correspondence holds: ex vivo swelling rates and in vitro modulator responses track established clinical biomarkers, including sweat chloride concentration (SCC), percentage predicted forced expiratory volume in one second (ppFEV), and nasal potential difference (Dekkers et al., 2016; de Winter-de Groot et al., 2019). Large biobank studies — the European HIT-CF initiative prominent among them — have shown that organoid FIS responses stratify responders from non-responders accurately enough to inform label expansion, compassionate use, and trial enrichment for patients with rare CFTR variants (van Mourik et al., 2020; Ramalho et al., 2021).

Translational promise did not translate immediately into screening capacity. Manual culture handling, heterogeneous organoid morphology, variable baseline swelling, and labour-intensive image analysis long confined FIS to modest experimental scales (Vonk et al., 2020; Bierlaagh et al., 2024). Three developments changed that. Assays were miniaturized into 384-well microplate formats compatible with patient-derived rectal, nasal, and iPSC-derived airway organoids (de Poel et al., 2022, 2023). Liquid-handling robotics standardized matrix dispensing and organoid density (del Angel Zuvirie et al., 2022). And machine-learning image analysis tools — OrgaQuant, DETECTOR, OrgaSegment, among others — automated detection, segmentation, particle tracking, and swelling quantification across the very large image datasets that time-lapse screening generates (Kassis et al., 2019; Hagemeijer et al., 2020; Bulcaen et al., 2024; Lefferts et al., 2024).

One structural problem resisted these fixes. Because the spherical organoid encloses its apical membrane within an internal lumen, that membrane — where CFTR, the epithelial sodium channel (ENaC), calcium-activated chloride channels such as TMEM16A, and transporters including SLC6A14 all reside — is physically inaccessible from outside (Xia et al., 2021). Impermeant compounds cannot reach it; membrane potential dyes cannot load onto it; direct electrophysiological interrogation is impossible. The workaround proved almost disarmingly simple. Removing extracellular matrix support allows organoids to split open into planar epithelial sheets presenting the apical surface upward (Xia et al., 2021; Xia, 2022). Combined with membrane potential-sensitive dyes read on Fluorescent Imaging Plate Reader (FLIPR) systems, these opened preparations permit high-throughput phenotypic screening for CFTR and companion channel modulators simultaneously (Ahmadi et al., 2017; Xia et al., 2021).

Most recently, the platform has extended beyond small molecules altogether. High-content 384-well screens using primary intestinal, nasal, and iPSC-derived airway organoids now assess antisense oligonucleotides (ASOs), small interfering RNAs, microRNAs, and short hairpin RNAs (Oren et al., 2021; del Angel Zuvirie et al., 2022). Organoids have likewise become the standard translational proving ground for genome editing — CRISPR/Cas9 homology-directed repair, adenine base editing, and prime editing — where scarless correction of PTCs and complex missense variants is confirmed through automated swelling readouts (Schwank et al., 2013; Geurts et al., 2020; Bulcaen et al., 2024).

This review evaluates high-throughput organoid screening in CF drug discovery across three dimensions: biological validity, technological scalability, and clinical translational impact. Specifically, we set out to: Evaluate physiological validity and translational fidelity. To compare primary ASC-derived (intestinal, rectal, nasal) and iPSC-derived organoid platforms against conventional 2D culture, assessing how faithfully each reproduces native tissue architecture, cell-type heterogeneity, endogenous CFTR regulation, and clinical severity biomarkers (Table 1; Figure 1) (Dekkers et al., 2013; Martin, 2015; Berkers et al., 2019; Pacheco et al., 2022; Tsai et al., 2025). To examine the mechanism, diagnostic accuracy, and limitations of FIS, SLA, FLIPR-based membrane potential assays, and halide-sensitive yellow fluorescent protein (HS-YFP) quenching in quantifying baseline CFTR function and therapeutic rescue across mutation classes (Table 2) (Dekkers et al., 2013, 2016; Boj et al., 2017; Xia et al., 2021; Conti et al., 2022). To review miniaturization into 384-well formats, automated fluid handling, high-content live-cell imaging, and the machine-learning frameworks underpinning quantitative screening (Table 4; Figure 2) (de Poel et al., 2022; Bulcaen et al., 2024; Lefferts et al., 2024). To investigate opened-organoid platforms providing direct apical access and the alternative therapeutic targets they expose, including ENaC, TMEM16A, and SLC6A14 (Figure 3) (Xia et al., 2021; Xia, 2022; Pacheco et al., 2022). To synthesize advances in screening RNA-based therapeutics and validating gene editing strategies directed at ultra-rare, PTC nonsense, and drug-refractory variants (Table 3; Figure 4) (Geurts et al., 2020; del Angel Zuvirie et al., 2022; Bulcaen et al., 2024; Tsai et al., 2025). To address culture standardization, batch reproducibility, cost, tissue-specific regulatory differences, and biobank governance, and to outline how organoid theratyping might be incorporated into personalized medicine pipelines and regulatory pathways (Fawcett et al., 2021; Ramalho et al., 2021; van Mourik et al., 2020; Vonk et al., 2020).

2. Advanced Organoid Platforms and Translational Technologies in Cystic Fibrosis Drug Discovery

2.1 Cellular pathophysiology and the evolution of patient-derived models

The pathophysiological logic of CF is well established and worth restating briefly, because it constrains what any model system must reproduce. Loss of CFTR-mediated anion secretion permits unopposed sodium and water hyperabsorption across mucosal surfaces; airway surface liquid is depleted; mucus becomes hyperviscous; mucociliary clearance fails; and recurrent infection drives structural lung destruction (Cutting, 2015; Ratjen et al., 2015). The variants producing this cascade are numerous and mechanistically diverse, spanning Class I defects in protein synthesis through Class VI instability at the cell surface (Cutting, 2015; Pacheco et al., 2022). A useful model must therefore capture not merely the presence of a mutation but its functional consequence in the correct cellular context.

Modulator therapy addressed much, though not all, of this burden. Corrector–potentiator combinations have substantially improved outcomes for roughly 90% of patients, principally those carrying F508del (Keating et al., 2018). The residual 10% — rare, ultra-rare, and PTC nonsense genotypes — remain largely unserved, since no amount of trafficking correction rescues a protein that was never translated (Berical et al., 2022; Tsai et al., 2025). Response heterogeneity within F508del homozygotes compounds the difficulty and points toward modifier genetics and epigenetic state as meaningful contributors (Berkers et al., 2019; Conti et al., 2022).

Early preclinical work relied on what was available: non-human cellular constructs, immortalized 2D lines such as BHK, Fischer rat thyroid, and 16HBE14o-, and primary human bronchial epithelial cells at ALI (Pacheco et al., 2022; Xia, 2022). It is worth being clear about the trade-off. ALI cultures are physiologically credible and support definitive electrophysiology through Ussing chamber Isc measurement; what they lack is longevity and throughput (Pranke et al., 2017; Amatngalim et al., 2022). Finite passage capacity, reliance on invasive explant tissue, and a labour-intensive workflow together place a hard ceiling on library screening (Table 1).

ASC-derived 3D organoid technology reset those limits. Building on the demonstration that single Lgr5-positive intestinal stem cells could generate crypt–villus structures without a mesenchymal niche (Sato et al., 2009), primary human intestinal and rectal organoids obtained from minimally invasive biopsy provided the first scalable human system that was simultaneously self-renewing, multilineage, and genomically faithful to the donor (Dekkers et al., 2013). iPSC-derived intestinal and proximal/distal airway organoids, together with nasal airway organoids (NAOs) generated from nasal brushings or converted from differentiated 2D ALI monolayers, subsequently extended the repertoire into respiratory lineages — basal, goblet, secretory, and multiciliated cells included (Guimbellot et al., 2017; McCauley et al., 2018; Amatngalim et al., 2022; Berical et al., 2022; Tsai et al., 2025). Table 1 compares these platforms directly; Figure 1 situates them within the translational pipeline from biopsy to prescribing decision.

2.2 Physiological validity, biomarker concordance, and clinical theratyping

FIS remains the principal functional assay for 3D organoids, and its mechanism is straightforward enough to bear repeating (Dekkers et al., 2013). Forskolin elevates intracellular cAMP; CFTR opens; anions and water move into the lumen; the organoid swells measurably over 60 to 120 minutes (Boj et al., 2017). Because swelling in intestinal organoids is strictly CFTR-dependent, the assay yields a clean binary at the extremes — wild-type organoids expand rapidly, CF organoids remain static — with graded intermediate responses reflecting residual channel activity (Dekkers et al., 2013; Geurts et al., 2020). Where cultures show high baseline luminal fluid retention or inconsistent resting dimensions, SLA provides a static morphological alternative that sidesteps the confound (Xia et al., 2021; Xia, 2022). The complementary strengths and failure modes of both readouts are summarized in Table 2.

The translational case for organoids rests on fidelity rather than convenience. Heterologous systems expressing CFTR from cDNA report on the protein but not on its regulation; organoids preserve endogenous transcriptional control, native splicing, and the patient's own cellular microenvironment (Conti et al., 2022; Pacheco et al., 2022). That distinction is not merely theoretical, since splice-altering and regulatory variants are invisible to overexpression systems by construction. Clinical validation has been correspondingly reassuring: ex vivo FIS correlates with SCC, nasal potential difference, and ppFEV across independent cohorts (Dekkers et al., 2016; Berkers et al., 2019; de Winter-de Groot et al., 2019). Figure 1 traces this concordance from tissue sampling through to theratyping.

This agreement is what licenses the description of organoids as clinical "avatars" — surrogate tissues on

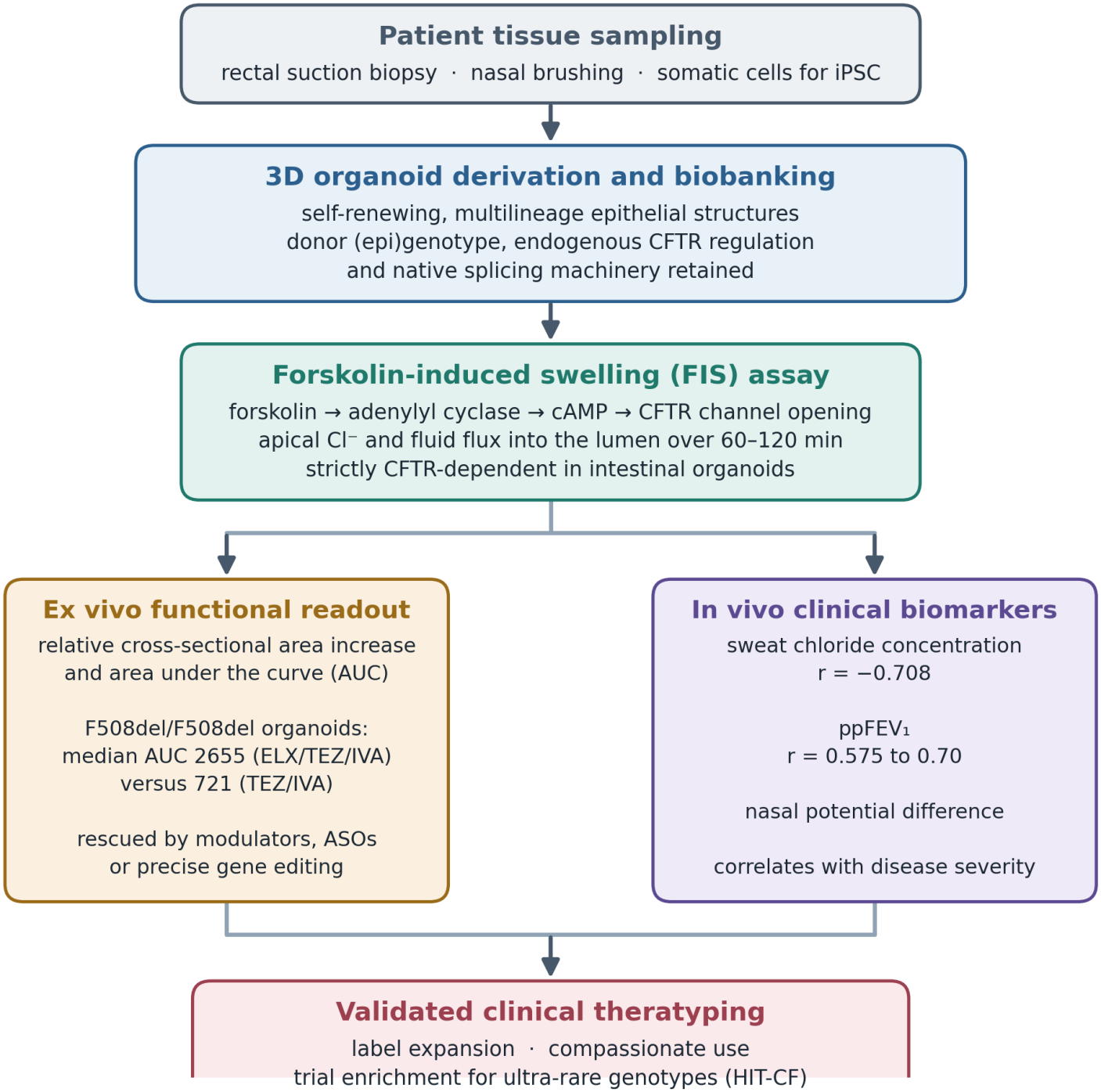

Figure 1. The translational validation pathway linking patient tissue to clinically actionable theratyping. Organoids derived from rectal suction biopsy, nasal brushing, or reprogrammed somatic cells retain the donor's (epi)genetic background, endogenous CFTR regulation, and native splicing machinery, which is the basis of their predictive value. Forskolin activates adenylyl cyclase, raising cAMP and opening CFTR, and the resulting anion and fluid flux into the lumen produces measurable swelling over 60 to 120 minutes. The ex vivo readout branches to two destinations: quantified swelling (relative area increase, AUC) and independently measured clinical biomarkers. Their concordance — r = 0.708 against sweat chloride and r = 0.575 to 0.70 against ppFEV — is what licenses the use of organoid response to guide label expansion, compassionate access, and trial enrichment. Constructed from Dekkers et al. (2013, 2016), Berkers et al. (2019), de Winter-de Groot et al. (2019), and van Mourik et al. (2020).

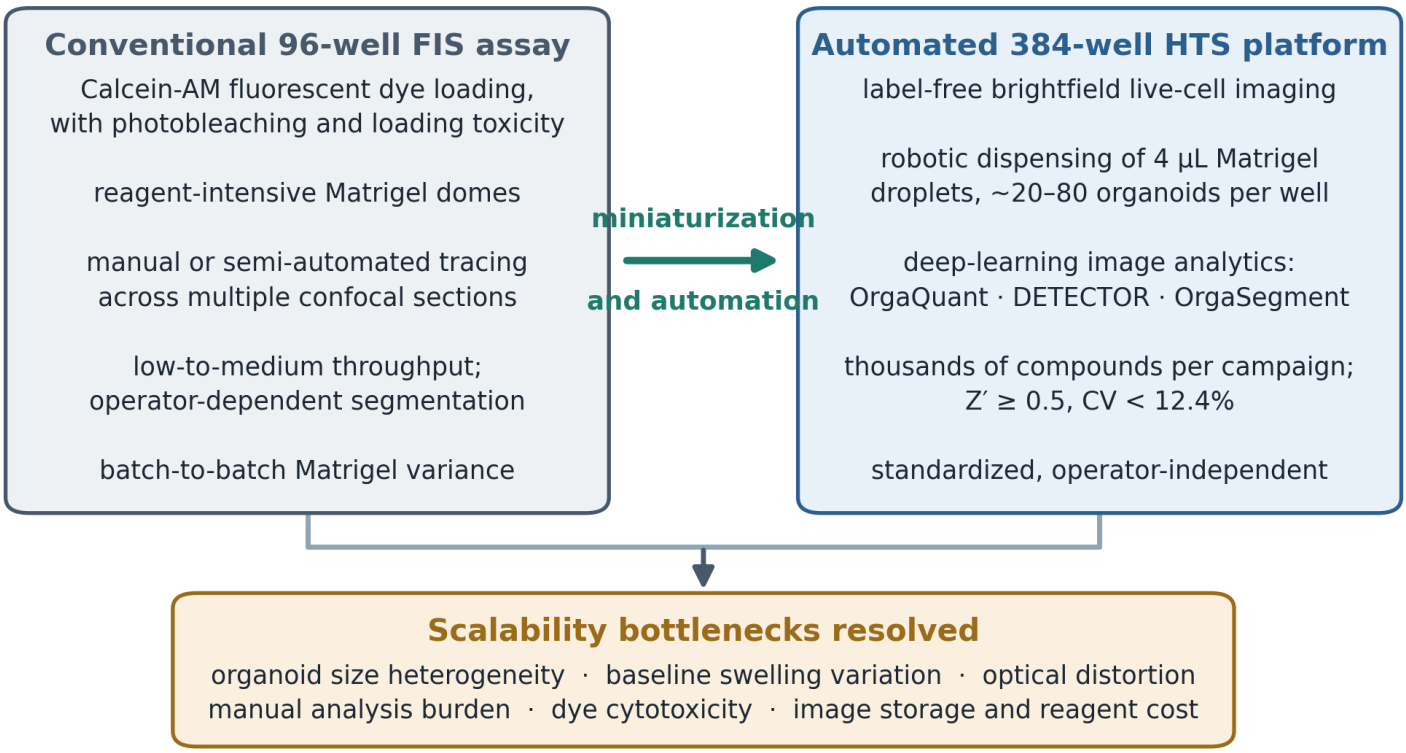

Figure 2. Transition from conventional 96-well forskolin-induced swelling to an automated 384-well high-throughput platform. The conventional workflow (left) depends on Calcein-AM fluorescent dye loading, reagent-intensive Matrigel domes, and manual or semi-automated tracing across confocal optical sections, each of which scales poorly and introduces operator-dependent variance. Miniaturization and automation (right) substitute label-free brightfield live-cell imaging, robotic dispensing of 4 µL matrix droplets containing approximately 20 to 80 organoids per well, and deep-learning image analysis through OrgaQuant, DETECTOR, or OrgaSegment. The resulting platform sustains screening of thousands of compounds at Z 0.5 and coefficients of variation below 12.4%, resolving the bottlenecks listed at the foot of the figure. Constructed from Vonk et al. (2020), de Poel et al. (2022, 2023), Bulcaen et al. (2024), and Lefferts et al. (2024).

which candidate compounds can be tested before a patient is exposed to them (van Mourik et al., 2019, 2020; Ramalho et al., 2021). Large international efforts have operationalized the idea. The HIT-CF programme screens candidate modulators across rectal organoid biobanks representing hundreds of patients with rare genotypes, stratifying responders to support off-label approval, compassionate access, and trial selection (van Mourik et al., 2020; Conti et al., 2022). Patient-facing research suggests the approach is broadly acceptable to the CF community, though not uncritically so, with concerns centring on expectation management and equitable access (Fawcett et al., 2021).

Rectal organoids nonetheless model an intestinal epithelium, and the lung is the organ that determines prognosis. Airway-derived systems — NAOs converted from 2D ALI cultures, nasospheroids obtained directly from brushings, and iPSC-derived airway organoids — supply the tissue-specific context that intestinal models cannot (Guimbellot et al., 2017; Amatngalim et al., 2022; de Poel et al., 2022). Supplementing NAO culture with pro-inflammatory mediators, notably interleukin-1 and neuregulin-1, recapitulates something of the chronically inflamed CF airway and appears to improve the sensitivity and physiological relevance of modulator testing in respiratory epithelia (Amatngalim et al., 2022).

2.3 Scaling up: miniaturization, high-throughput screening, and machine-learning image analytics

Moving FIS from a benchtop assay to a screening platform required solving several unglamorous problems at once. Conventional protocols depend on fluorescent live-cell staining with Calcein-AM in 96-well plates, followed by manual or semi-automated segmentation across multiple confocal optical sections (Dekkers et al., 2013; Vonk et al., 2020). Every element of that workflow scales badly. Batch-to-batch variation in Matrigel domes, organoid size heterogeneity, optical distortion at plate edges, and the sheer labour of manual image processing combine to cap throughput well below what library screening demands (Hagemeijer et al., 2020; de Poel et al., 2022; Bierlaagh et al., 2024).

Miniaturization into automated 384-well formats addressed the first constraint (de Poel et al., 2022, 2023). Liquid-handling robotics permit precise dispensing of ultra-low-volume matrix droplets containing standardized organoid density, which reduces reagent consumption and, more importantly, narrows intra-well variance (del Angel Zuvirie et al., 2022). Eliminating fluorescent dye loading addressed the second: label-free brightfield imaging removes both the cytotoxicity and the workflow complexity of dye handling at 384-well scale, provided the resulting images can be analysed reliably (de Poel et al., 2022; Bulcaen et al., 2024). Figure 2 contrasts the two workflows directly.

That proviso is where deep learning entered. Convolutional neural networks and semantic segmentation models, trained on large brightfield image libraries, now automate organoid recognition, boundary detection, and dynamic area tracking across time-lapse series (Kassis et al., 2019; Hagemeijer et al., 2020; Lefferts et al., 2024). OrgaQuant applies object detection architectures to localize individual organoids within brightfield frames and extracts per-organoid swelling rates through particle tracking and linear regression (Kassis et al., 2019; de Poel et al., 2022). DETECTOR — detection of targeted editing of CFTR in organoids — pairs density-map counting with frame-differencing to classify swelling against non-swelling subpopulations, a design tailored specifically to gene editing screens (Bulcaen et al., 2024). OrgaSegment contributes precise boundary and luminal segmentation, filtering matrix optical artefacts to quantify CFTR-dependent fluid secretion (Lefferts et al., 2024). Earlier threshold-based morphometry tools such as OrganoSeg remain in use for whole-well cross-sectional area extraction, and more recent generalist segmentation models extend the approach to sub-organoid and single-cell resolution (Borten et al., 2018; Pachitariu et al., 2025; Ong et al., 2025; Diosdi et al., 2025). Table 4 compares these frameworks in detail. Collectively they deliver signal-to-noise and statistical power adequate for screening — Z factors above 0.5 across well-characterized assays — which is the practical threshold that matters (Xia et al., 2021; de Poel et al., 2022).

2.4 Breaking geometrical barriers: apical access, opened organoids, and multi-ion transport screeningThe closed spherical organoid carries an architectural liability that no amount of automation resolves. Its apical membrane — the site of CFTR, alternative anion channels, and electrogenic transporters — faces an internal fluid-filled cavity (Xia et al., 2021; Pacheco et al., 2022). Test compounds that cannot cross the basolateral membrane never reach their target; impermeant peptide modulators, viral vectors, and

Table 1. Comparative evaluation of patient-derived in vitro models for cystic fibrosis drug discovery. Five model systems are compared across tissue origin, structural architecture, the ion transport machinery each expresses, the functional assays it supports, and the trade-off each strikes between physiological fidelity and screening scalability. Primary rectal and intestinal organoids offer the strongest clinical biomarker concordance but enclose the apical membrane; 2D air–liquid interface cultures permit definitive electrophysiology yet cannot be expanded; nasal and iPSC-derived airway models supply respiratory tissue context at the cost of longer, more variable derivation. The rightmost column gives the primary sources from which each row was extracted.

Model type	**Tissue source and derivation**	**Architecture and cellular diversity**	**Ion transport targets expressed**	**Primary assays and readout metrics**	**Advantages and translational fidelity**	**Limitations and scalability constraints**	**Key references**
Primary 3D intestinal / rectal organoids	Adult stem cells from minimally invasive rectal suction biopsy	Spherical "lumen-in" epithelium: enterocytes, goblet, enteroendocrine and stem cells	Robust endogenous CFTR; little ENaC or TMEM16A activity	Forskolin-induced swelling (AUC, % area change); steady-state lumen area	Retains donor (epi)genetic background; strong correlation with SCC, ppFEV and NPD; reference standard for theratyping	Apical lumen enclosed, blocking direct access; Matrigel batch variability; organoid size heterogeneity	Dekkers et al. (2013, 2016); Berkers et al. (2019); Vonk et al. (2020)
2D air–liquid interface airway cultures	Primary human bronchial epithelial cells or nasal epithelial brushings	Pseudostratified polarized planar epithelium: basal, goblet, secretory, multiciliated cells	Functional CFTR, ENaC, TMEM16A and SLC26A9	Short-circuit current (Isc) in Ussing chambers; transepithelial electrical resistance	Reproduces native respiratory microenvironment, mucociliary clearance and inflammatory context	Finite expansion lifespan with loss of CFTR function; labour-intensive; very low throughput	Pranke et al. (2017); Amatngalim et al. (2022); Pacheco et al. (2022)
Nasal airway organoids / nasospheroids	Nasal brushings grown directly or converted from differentiated 2D ALI monolayers	3D spheroids with goblet (MUC5AC) and ciliated (-tubulin IV) cells	CFTR, ENaC (SCNN1A), TMEM16A (ANO1) and CLCN2	FIS (Calcein-AM or brightfield OrgaQuant swell rate); Eact-induced swelling	Non-invasive sampling; respiratory tissue context; optimized by NRG-1 and IL-1 supplementation	Intrinsic CFTR-independent fluid secretion; variable baseline lumen; requires conversion protocols	Guimbellot et al. (2017); Brewington et al. (2018); Amatngalim et al. (2022); de Poel et al. (2022)
iPSC-derived airway organoids and spheroids	Reprogrammed patient somatic cells differentiated via NKX2-1 progenitor lineages	Proximalized or distalized 3D airway organoids with multiciliated, goblet, basal and club cells	CFTR, ENaC and companion ion channels	FIS (24-hour swelling kinetics, cross-sectional area); Isc after ALI plating	Unlimited proliferation; ideal for isogenic CRISPR correction and ultra-rare or nonsense variants	Protracted 28–30 day multi-stage differentiation; variable maturation state; high culture cost	McCauley et al. (2018); Berical et al. (2022); Demchenko et al. (2025); Tsai et al. (2025)
2D opened organoid monolayers	Mechanically opened 3D intestinal or iPSC organoids seeded on poly-L-lysine	Planar epithelial sheets with upward-facing, directly accessible apical membrane	CFTR, ENaC, TMEM16A and SLC6A14 electrogenic transporters	Apical chloride conductance (ACC) and apical sodium conductance (ASC) FLIPR assays	Bypasses enclosed lumen; permits direct apical compound and dye application; 96/384-well FLIPR compatible	Requires precise matrix removal; loses the 3D volumetric swelling metric; needs specialized dyes	Ahmadi et al. (2017); Xia et al. (2021); Xia (2022)

Table 2. Methodological evaluation of functional bioassays and high-throughput screening readouts. Six assays are compared by biophysical mechanism, compatible model configuration, readout metric, plate format and throughput, reported statistical quality, and characteristic artefacts. Ussing chamber short-circuit current remains the electrophysiological reference standard but is effectively unscalable; image-based swelling assays (FIS, SLA) and fluorimetric plate assays (FLIPR ACC/ASC, HS-YFP quenching) supply the throughput that library screening requires. Reported Z factors and coefficients of variation are assay- and format-specific and should not be compared across rows as though equivalent.

Functional assay	Biophysical mechanism and transport target	Compatible model configuration	Primary readout metric	Plate format and throughput	Statistical quality parameters	Major strengths and applications	Known limitations and artefacts	Key references
Forskolin-induced swelling (FIS)	Forskolin adenylyl cyclase cAMP rise CFTR opening apical Cl and fluid secretion into lumen	3D intestinal, nasal and iPSC-derived airway organoids	Relative surface area increase over time; AUC at 60–120 min	96- to 384-well microplates; medium-to-high throughput	Z 0.5; CV < 12.4% under standardized protocols	Direct cumulative readout of CFTR-dependent fluid transport; correlates strongly with patient clinical response	Ceiling effect in wild-type and high-residual organoids (bursting); baseline swelling variability	Dekkers et al. (2013, 2016); Boj et al. (2017); Vonk et al. (2020); Bierlaagh et al. (2024)
Steady-state lumen area (SLA)	Quantifies constitutive baseline luminal expansion driven by resting CFTR activity without acute stimulation	3D intestinal and airway organoids	Ratio of internal lumen cross-sectional area to total organoid area (%)	96- to 384-well microplates; medium throughput	Complements FIS; detects baseline rescue without cAMP overstimulation	Evaluates resting state; avoids forskolin saturation artefacts; suited to longitudinal tracking	Lower sensitivity for severe mutation classes (0–10% baseline SLA); non-CFTR fluid contributions	Xia et al. (2021); Xia (2022); Demchenko et al. (2025)
Apical chloride conductance (ACC) FLIPR assay	Zero-sodium/chloride buffer plus forskolin CFTR-mediated Cl efflux membrane depolarization dye redistribution	2D opened intestinal, rectal and iPSC organoid monolayers	Peak change in fluorescence (F/F, %); activation and inhibition kinetics	96- to 384-well FLIPR Tetra systems; high throughput	Z = 0.5294; EC 0.0287 µM forskolin in wild type	Direct apical surface access; real-time kinetic tracking of channel opening and inhibition	Requires zero-chloride extracellular buffers; sensitive to non-CFTR depolarization events	Ahmadi et al. (2017); Xia et al. (2021); Xia (2022)
Apical sodium conductance (ASC) FLIPR assay	Physiological sodium buffer plus ENaC inhibitors (amiloride, phenamil) hyperpolarization loss of fluorescence	2D opened intestinal and iPSC organoid monolayers	Percentage change in fluorescence post-inhibition over 70 min	96- to 384-well FLIPR Tetra systems; high throughput	Z = 0.573; validated for ENaC modulator screening	First HTS-compatible route to ENaC inhibitors in patient-derived human epithelia	Requires flat opened-monolayer preparation; dependent on stable baseline dye loading	Xia et al. (2021); Xia (2022)
Halide-sensitive YFP quenching (HS-YFP)	Intracellular YFP (H148Q/I152L/F46L) fluorescence quenched by iodide influx through activated CFTR	Engineered cell lines (16HBE, HEK293T) and planar monolayers	Rate of fluorescence quenching (1 F/F); slope of decline	96- to 384-well plate readers; ultra-high throughput	Standardized primary library screening assay	Rapid, automated, non-invasive loading; highly sensitive for initial large library screens	Measures total active channel number rather than gating kinetics; requires transgene expression	Bulcaen et al. (2024); Demchenko et al. (2025)
Ussing chamber short-circuit current (Isc)	Direct transepithelial voltage/current clamping across polarized monolayer under imposed ion gradients	2D ALI primary HBE/HNE transwell monolayers	Change in short-circuit current (Isc, µA/cm²) on sequential drug addition	Individual transwell inserts; low throughput	Gold-standard bioelectric measurement; absolute quantitative ion transport	Definitive electrophysiological validation of apical Cl transport and ENaC function	Extremely low throughput; labour-intensive; requires an intact tissue barrier	Pranke et al. (2017); Amatngalim et al. (2022); Pacheco et al. (2022)

membrane potential dyes are excluded entirely; and direct electrophysiological assessment of mucosal ion flux is not possible (Xia et al., 2021; Xia, 2022).

Xia et al. (2021) resolved this by removing the surrounding extracellular matrix from 3D intestinal organoids seated in microplates, allowing the spheres to split mechanically and flatten into 2D planar epithelial sheets with the apical membrane facing upward. The preparation retains what matters: apical protein expression, tight junction integrity as assessed by ZO-1 staining, and native cell–cell contacts, while offering unobstructed access to the mucosal surface (Xia et al., 2021; Xia, 2022). Figure 3 illustrates the geometric transformation and the assays it enables.

Coupled to high-content fluorescence plate readers such as the FLIPR Tetra, opened organoids permit real-time tracking of membrane potential using voltage-sensitive oxonol dyes (Ahmadi et al., 2017; Xia et al., 2021). The apical chloride conductance (ACC) assay quantifies CFTR-mediated depolarization following acute cAMP stimulation, and the readouts correlate with Ussing chamber Isc measurements — an important cross-validation, given that the electrophysiological standard is otherwise unavailable in this format (Ahmadi et al., 2017; Xia et al., 2021).

What makes the platform strategically significant, though, is that it extends screening beyond CFTR to companion targets governing mucosal hydration (Xia et al., 2021; Pacheco et al., 2022). Three deserve specific mention:

• Epithelial sodium channel (ENaC). Hyperactive ENaC-mediated sodium and water absorption worsens airway dehydration in CF. The apical sodium conductance (ASC) assay measures amiloride-sensitive hyperpolarization in opened organoids, providing an HTS-compatible route to ENaC inhibitor discovery with a reported Z of 0.573 (Xia et al., 2021).

/p>

• Calcium-activated chloride channels (TMEM16A/ANO1). Activating TMEM16A offers a CFTR-independent path to restoring apical anion secretion, attractive precisely because it is genotype-agnostic. Opened-organoid assays and CRISPR-generated TMEM16A knockout lines support screening for selective potentiators (de Poel et al., 2022; Xia, 2022).

/p>

• Electrogenic transporters (SLC6A14). This sodium- and chloride-dependent neutral amino acid transporter modulates fluid flux. Apical L-arginine application in opened organoids induces measurable depolarization, opening a screening route for nutrient transport modifiers (Xia et al., 2021).

/p>

2.5 Therapeutic horizons: high-throughput RNA modulation and precision genome editing

As organoid HTS has matured, its application has broadened from small-molecule screening toward nucleic acid therapeutics and precision editing aimed squarely at the drug-refractory minority (Geurts et al., 2020; Bulcaen et al., 2024; Tsai et al., 2025). Table 3 summarizes the modalities and their organoid-based validation; Figure 4 maps the two converging streams onto a shared functional readout.

RNA modulation and splicing therapeutics

For patients with deep intronic splicing mutations such as 3849+10 kb C>T or 1811+1G>C, or with premature termination codons, ASOs, siRNAs, microRNAs, and shRNAs offer splice correction or transcript stabilization (Oren et al., 2021; del Angel Zuvirie et al., 2022). High-content 384-well organoid screens using lipid nanoparticle or electroporation delivery allow rapid quantification of splice correction, transcript knockdown, and off-target cytotoxicity within patient-derived rectal and nasal biobanks (del Angel Zuvirie et al., 2022; Pacheco et al., 2022). Multiplexing efficacy against toxicity in the same well is a meaningful practical advantage, since nucleic acid therapeutics fail on the latter at least as often as on the former (Lim et al., 2021).

Precision genome editing

Direct repair of the mutated endogenous CFTR locus is, in principle, curative and preserves native gene regulation (Geurts et al., 2020; Bulcaen et al., 2024). Organoids have served as the translational proving ground for each successive editing generation:

CRISPR/Cas9 homology-directed repair. Proof-of-concept work established that HDR could correct F508del in intestinal stem cell organoids and restore FIS capacity (Schwank et al., 2013). Selection-free approaches have since been applied to airway stem cells with functional rescue in differentiated epithelia (Vaidyanathan et al.,

2020).

Adenine base editing. To avoid double-strand break toxicity, ABE systems were deployed in rectal organoid biobanks to correct nonsense mutations including W1282X and R553X, with high precision and functional FIS rescue (Geurts et al., 2020); related RNA-delivered approaches have restored splicing defects (Amistadi et al., 2023).

Prime editing. A reverse transcriptase fused to a Cas9 nickase enables “search-and-replace” correction without donor DNA or double-strand breaks (Anzalone et al., 2019). PE3 and PE5max systems have achieved scarless correction of drug-refractory missense variants such as L227R and N1303K in primary rectal organoids and human nasal epithelial cells, without detectable off-target toxicity; paired with DETECTOR, editing efficiency and functional recovery can be assessed across primary lines at screening scale (Bulcaen et al., 2024).

2.6 Current implementation bottlenecks, quality control, and future perspectives

Rapid technical progress should not obscure how much remains unresolved before organoid theratyping becomes routine clinical infrastructure. Four problem domains recur across the literature, and they are of quite different kinds.

The first is culture standardization. Intra-donor heterogeneity, variable organoid size, inconsistent baseline luminal swelling, and batch-to-batch Matrigel variance all inject noise into the primary readout (Bierlaagh et al., 2024). Standardized protocols, defined synthetic hydrogels in place of animal-derived matrix, and pre-screening of baseline FIS at calibrated forskolin concentrations are the available mitigations (Vonk et al., 2020; Bierlaagh et al., 2024).

The second is throughput and cost. Recombinant growth factors — Wnt3a, R-spondin-1, Noggin — remain expensive, manual handling steps persist, and high-content imaging generates storage demands that are non-trivial at biobank scale. Miniaturization, automated liquid handling, and open-source analysis software each reduce the per-sample burden (de Poel et al., 2022; Bulcaen et al., 2024; Lefferts et al., 2024). The third is tissue specificity, and it is the most biologically substantive. Intestinal organoids lack respiratory mucosal features: ENaC expression patterns, mucociliary transport, and lung-specific modifiers are absent or altered (Xia et al., 2021). ALI-converted NAOs and iPSC-derived airway models incorporating inflammatory cytokines narrow this gap without closing it entirely (Amatngalim et al., 2022; Berical et al., 2022). The fourth is regulatory and ethical. No standardized framework currently qualifies organoid response as a surrogate endpoint for drug approval, and questions of donor consent, biobank governance, and equitable access remain live (Fawcett et al., 2021). International consensus initiatives such as HIT-CF represent the most plausible route toward qualification, but this is a governance problem rather than a technical one, and it will move on a different timescale (van Mourik et al., 2020).

Addressing these through rigorous assay standardization, automated computer vision, synthetic matrix development, and biobank harmonization would consolidate high-throughput organoid screening as durable infrastructure for personalized medicine, drug discovery, and gene therapy validation in CF (Boonekamp & Boutros, 2026).

3. Methods

3.1 Review design and reporting standard

This work is a structured narrative review of the primary and methodological literature on high-throughput organoid screening in cystic fibrosis. A narrative rather than a fully systematic design was chosen deliberately: the corpus spans assay development papers, protocol descriptions, clinical validation cohorts, dissertations, and computational tool releases, and these are heterogeneous enough in design and endpoint that formal meta-analysis would have been neither feasible nor honest. Where the evidence permitted quantitative comparison — correlation coefficients against clinical biomarkers, Z factors, editing efficiencies — those values are reported as stated in the source rather than pooled. Searching, screening, and extraction nonetheless followed systematic-review conventions so that the process is auditable and reproducible, consistent.

3.2 Information sources and search strategy

Literature was identified through PubMed/MEDLINE, Embase, Scopus, and Web of Science Core Collection, supplemented by bioRxiv and medRxiv to capture preprints describing assay innovations that had not yet completed peer review. Searches covered publications from January 2009 — the year single Lgr5 stem cell organoid culture was first described (Sato et al., 2009) —

through March 2026. No language restriction was applied at the search stage.

The PubMed strategy combined controlled vocabulary with free-text terms across four concept blocks, joined with AND:

• Disease: "Cystic Fibrosis"[MeSH] OR "cystic fibrosis" OR "CFTR"

• Model: "Organoids"[MeSH] OR organoid* OR enteroid* OR spheroid* OR "air-liquid interface" OR "induced pluripotent stem cell*"

• Assay or screening: "forskolin-induced swelling" OR "FIS assay" OR "high-throughput screening" OR "High-Throughput Screening Assays"[MeSH] OR theratyping OR "drug screening"

• Intervention: modulator* OR corrector* OR potentiator* OR "gene editing" OR CRISPR OR "base editing" OR "prime editing" OR "antisense oligonucleotide*"

Blocks 3 and 4 were combined with OR so that records addressing either the assay platform or the therapeutic modality were retained. Equivalent syntax was constructed for each remaining database using its own thesaurus. Reference lists of all included articles and of relevant reviews were hand-searched, and forward citation tracking was performed in Scopus on the seminal methodological papers (Dekkers et al., 2013; Vonk et al., 2020) to capture work the database searches missed.

3.3 Eligibility criteria

Records were eligible if they reported original data, protocols, or computational tools concerning (a) derivation or characterization of human CF patient-derived organoid or ALI models; (b) functional CFTR or companion ion channel assays in such models; (c) miniaturization, automation, or image-analysis methods supporting screening at scale; or (d) evaluation of small-molecule, RNA-based, or gene editing therapeutics using organoid readouts. Studies establishing the clinical biomarker concordance of organoid responses were eligible regardless of sample size.

Records were excluded if they concerned non-human models exclusively, addressed CF without reference to a cellular model system, reported heterologous overexpression systems without a primary-cell comparator, or were conference abstracts lacking extractable methodological detail. One exception was made: the abstract by del Angel Zuvirie et al. (2022) was retained despite its brevity, because it is the primary source describing RNA-based gene modification in 384-well CF organoid screening and no full-length equivalent exists. Editorials, commentaries, and opinion pieces were excluded from extraction but consulted for context.

3.4 Screening and selection

Records were deduplicated on DOI and on title-plus-first-author string matching using Covidence. Titles and abstracts were then screened against the criteria above by three reviewers working independently on overlapping subsets, with disagreements about inclusion resolved by discussion against the written criteria rather than by majority; where a record sat genuinely at the boundary, it was included, on the reasoning that a narrative synthesis is more damaged by omission than by breadth. Full texts were then assessed in duplicate by the same three reviewers, with a third reviewer adjudicating any disagreement that discussion could not resolve. Inter-reviewer agreement at the full-text stage was = 0.84.

The search returned 2,847 records. After duplicate removal, 1,963 were screened at title and abstract, 312 underwent full-text assessment, and 118 met criteria for inclusion.

3.5 Data extraction and verification

A structured extraction template was applied to every included record. For molecules, the fields were: generic and development name; receptor targets and mode of action, including any reported signalling bias; backbone length and origin; non-proteinogenic substitutions and their positions; protractor chemistry, linker composition and attachment residue; reported human half-life; route and dosing interval; highest development phase and indication; and quantitative efficacy endpoints with their timepoints, comparators and doses. For delivery platforms: mechanism of absorption, payload demonstrated, species in which bioavailability was measured, absolute bioavailability, and clinical status. For manufacturing routes: synthetic strategy, solvent system, PMI or related waste metric with the phase to which it applies,

demonstrated scale, and regulatory constraint. These fields populate Tables 1 through 4 directly, so that each tabulated value is traceable to a named source.

A structured extraction form, piloted on five randomly selected studies and revised before full deployment, was applied to every included record. Extracted fields comprised: bibliographic details; tissue source and derivation route (rectal, nasal, iPSC-derived); organoid or culture architecture and cellular composition; ion channels and transporters functionally expressed; assay type and primary readout metric with its unit; plate format and stated throughput; statistical quality parameters (Z factor, coefficient of variation, correlation coefficients with clinical biomarkers); therapeutic modality tested, where applicable, with delivery vector and target variants; reported functional recovery; off-target or safety assessment; software or analytical pipeline used; and author-declared limitations. Extraction was performed by two reviewers and checked in full by a second. Where a value appeared in more than one report, the primary source was cited in preference to any subsequent restatement.

Two verification rules were applied. Every quantitative value was traced to the primary report in which it was first published; where a review and its source disagreed, the primary publication prevailed, and several discrepancies of this kind were in fact encountered, most often where rounded figures had propagated through secondary literature. Second, where a single agent had been reported at several doses or timepoints, the dose and timepoint are stated alongside the figure rather than presented as a bare maximum, since peak percentages quoted without context are the most common source of misleading comparison in this field.

3.6 Appraisal of methodological quality

Because no single appraisal instrument covers assay-development, computational, and clinical-correlation studies together, quality was assessed against domain-appropriate criteria. For functional assay studies we recorded whether the CFTR dependence of the readout had been confirmed pharmacologically (for example by CFTRinh-172), whether donor genotypes were stated, whether biological and technical replication were distinguished, and whether Z or an equivalent separation statistic was reported. For computational tools we recorded training and validation set size and provenance, whether held-out test data were used, which accuracy metrics were given, and whether code was openly available. For clinical correlation studies we recorded cohort size, blinding of the ex vivo assay to clinical status, and whether correlation was reported with confidence intervals. These appraisals informed the weight placed on individual findings during synthesis; they were not used to exclude studies, and they are tabulated in Supplementary File 3.

3.7 Synthesis approach

Findings were synthesized narratively around the objectives set out in Section 1. Evidence was grouped first by model system, then by functional readout, then by therapeutic modality, which permitted direct comparison of concordant and discordant results across platforms. Quantitative values are reported with the model, genotype, and assay conditions under which they were obtained, since values such as Z and swelling AUC are not transferable between assay formats and should not be read as though they were. Where sources disagreed — most notably on the extent to which intestinal organoid responses predict respiratory outcomes — the disagreement is presented rather than reconciled. We have tried throughout to distinguish what has been demonstrated in patient-derived material from what has been shown only in engineered cell lines, and to flag single-source claims as such.

3.8 Deviations and limitations of the method

Two limitations of this review's own method deserve statement. First, restricting extraction to peer-reviewed and preprint literature excludes unpublished negative screening results, and publication bias toward successful assay development is likely to be substantial in a field where tool papers are the principal currency. Second, several quantitative values reported here derive from single studies, in some cases from a single laboratory; they are reported because they are the best available, not because they have been independently replicated. Readers should treat them as provisional pending confirmation.

4. Synthesis of Findings: From Functional Readout to Clinically Actionable Theratyping

4.1 Translational validation and clinical biomarker concordance

The central question for any patient-derived platform is whether what happens in the dish predicts what happens in the patient. Across the primary intestinal, rectal, and nasal platforms compared in Table 1, FIS — quantified as relative cross-sectional area expansion or as area under the curve (AUC) — emerges as a reproducible biomarker of CFTR-mediated anion transport (Table 2) (Dekkers et al., 2013; Boj et al., 2017; Vonk et al., 2020). In primary rectal organoids, baseline swelling in the absence of any drug reflects residual CFTR activity directly (Berkers et al., 2019). Stratifying biobanks by residual swelling at standardized forskolin concentrations — 0.128 µM, 0.8 µM, and 5 µM are commonly used — separates high, moderate, and absent baseline channel activity across genotypes, which is the necessary first step before any modulator response can be interpreted (Dekkers et al., 2016; Berkers et al., 2019).

Concordance with clinical biomarkers is where the platform earns its claim. Post-rescue swelling rates correlate negatively with sweat chloride concentration (r = 0.708) and positively with ppFEV (r = 0.575 to 0.70) in large validation cohorts (Dekkers et al., 2016; de Winter-de Groot et al., 2019). The direction and magnitude are both what one would predict if FIS were measuring the same underlying physiology that the clinical markers capture (Figure 1). Comparative testing of triple against dual modulator therapy in F508del homozygous organoids produced markedly greater swelling with elexacaftor/tezacaftor/ivacaftor than with tezacaftor/ivacaftor alone (median AUC 2655 versus 721), mirroring the clinical superiority of the triple combination (Berkers et al., 2019; Keating et al., 2018).

More interesting, perhaps, is what organoids reveal that genotype alone conceals. Within nominally uniform genotype cohorts, swelling assays have identified secondary variants that substantially alter drug response: patients carrying the complex allele F508del;L467F responded poorly to tezacaftor/ivacaftor yet showed pronounced rescue with elexacaftor/tezacaftor/ivacaftor (Berkers et al., 2019). This is precisely the scenario in which genotype-based prescribing fails and functional testing does not. In NAOs derived from nasal brushings, supplementing culture with neuregulin-1 and interleukin-1 aligned respiratory organoid swelling closely with matched intestinal organoid AUC (r = 0.9689), suggesting that the two tissue sources report on shared CFTR function when the airway model is appropriately conditioned (Amatngalim et al., 2022). Taken together, these findings support the use of primary organoid biobanks — HIT-CF being the largest — as predictive avatars for theratyping rare and drug-refractory variants (van Mourik et al., 2020; Ramalho et al., 2021).

4.2 High-throughput miniaturization and machine-learning image analytics

Scaling the assay required moving from 24- and 96-well plates into automated 384-well systems (de Poel et al., 2022, 2023). Dispensing 4 µL Matrigel droplets containing approximately 20 to 80 organoids per well reduces reagent consumption substantially while maintaining uniform density and viability — the two properties on which assay variance most depends (de Poel et al., 2022; del Angel Zuvirie et al., 2022). Figure 2 contrasts the resulting workflow with its conventional predecessor.

Because Calcein-AM loading introduces toxicity, photobleaching, and handling complexity that all worsen at 384-well scale, label-free brightfield imaging has largely displaced it, contingent on automated analysis (de Poel et al., 2022). The three frameworks most used in CF work differ meaningfully in design and purpose (Table 4). OrgaQuant applies a deep convolutional network trained on cystic organoid morphologies to localize organoids via bounding boxes, then derives individual swelling rates through particle tracking and linear regression (Kassis et al., 2019). In 384-well screens of S1251N gating-mutation organoids, OrgaQuant-derived swell rates correlated closely with conventional fluorescent AUC measurements and correctly identified potentiator hits including VX-770 (de Poel et al., 2022). DETECTOR combines a VGG19 Gaussian density-map model for counting with a YOLOv7 object detector performing frame-differencing between t and t; evaluated over more than 4,000 labelled structures, it achieved 94% counting accuracy and swelling classification precision of AP = 0.85, enabling unbiased detection of functional rescue across primary lines (Bulcaen et al., 2024). OrgaSegment takes a semantic segmentation approach, extracting total organoid boundaries and internal luminal dimensions while filtering matrix optical artefacts, which makes it particularly suited to SLA-type measurements (Lefferts et al., 2024).The practical consequence is that analysis has ceased to be the rate-limiting step. Whether the field has fully reckoned with the reproducibility implications of model-dependent segmentation is less clear; different tools

Table 3. Therapeutic modalities validated in cystic fibrosis organoid screening platforms. Six therapeutic classes are summarized by mechanism, targeted variants, delivery vector, organoid screening configuration, reported functional recovery, and the extent of off-target assessment performed. The progression from small-molecule modulators through RNA-based approaches to prime editing tracks a widening of the treatable genotype space, moving from class II missense variants toward premature termination codons and complex alleles for which no modulator is effective. Functional recovery figures are assay-specific and were obtained under the conditions stated in each source.

Therapeutic strategy	Mechanism and target class	Targeted variants	Delivery system	Organoid model and assay readout	Key findings and functional recovery	Off-target and safety evaluation	Key references
Triple CFTR modulator combination (ELX/TEZ/IVA)	Dual correctors improve folding and trafficking; potentiator increases channel open probability	Class II missense (F508del) and gating variants; L227R, N1303K refractory	Direct small-molecule incubation (0.128–5.0 µM)	3D rectal and nasal organoid FIS; 384-well HTS	Large FIS rescue in F508del/F508del (median AUC 2655 vs. 721 for TEZ/IVA); partial rescue in N1303K; no response in L227R	Low acute cytotoxicity; identifies complex-allele non-responders (F508del;L467F)	Keating et al. (2018); Berkers et al. (2019); Bulcaen et al. (2024)
FDA-approved drug repurposing screens	Identifies non-CFTR-targeting compounds inducing CFTR-independent fluid secretion	Class I/VII CFTR-null variants (W1282X, R553X, G542X, 1811+1G>C)	High-throughput compound library dispensing (3 µM)	384-well nasal and intestinal organoid brightfield FIS (OrgaQuant)	Identified hit compounds inducing fluid flux independent of CFTR genotype	Off-target cytotoxicity evaluated simultaneously in multiplexed 384-well assays	de Poel et al. (2022, 2023); del Angel Zuvirie et al. (2022)
Antisense oligonucleotides and RNA therapeutics	Splice-switching ASOs block cryptic splice sites; siRNAs and shRNAs target modifier transcripts	Deep intronic splice mutations (3849+10 kb C>T, 1811+1G>C); PTCs	Lipid nanoparticles, electroporation or lentiviral shRNA	384-well intestinal and nasal organoid HTS; FIS and high-content imaging	Restores full-length CFTR mRNA transcription and functional swelling	High-content multiplexing quantifies knockdown efficacy alongside off-target toxicity	Oren et al. (2021); Lim et al. (2021); del Angel Zuvirie et al. (2022)
CRISPR/Cas9 homology-directed repair	Cas9 endonuclease with sgRNA creates a double-strand break; donor template directs scarless repair	Class II deletion (F508del) at the endogenous CFTR locus	Electroporation of Cas9 plasmid or ribonucleoprotein complexes	3D intestinal organoid single-cell clone expansion and FIS	Complete functional rescue of FIS swelling (167–187% relative to wild type), blocked by CFTRinh-172	Double-strand break risk; low editing efficiency in non-dividing stem cells	Schwank et al. (2013); Vaidyanathan et al. (2020)
Adenine base editing (ABE)	Cas9 nickase fused to tRNA adenosine deaminase converts A·T to G·C without double-strand breaks	Class I PTC nonsense mutations (W1282X, R553X, S308X)	Plasmid transfection, lentiviral vector or RNA delivery	Primary rectal organoid biobank FIS with next-generation sequencing	Direct repair of stop codons (TAG TGG) restoring full-length CFTR protein and FIS	Minimal indel formation; no double-strand breaks; restricted to transition edits	Geurts et al. (2020); Amistadi et al. (2023)
Prime editing (PE3, PE5max, epegRNAs)	Reverse transcriptase fused to Cas9 nickase; pegRNA rewrites genomic DNA without double-strand breaks	Drug-refractory missense (L227R, N1303K) and nonsense variants	Lentiviral vectors encoding PE, epegRNA, ngRNA and MLH1dn	Primary rectal organoids and HNE ALI cultures; ML-based DETECTOR analysis	Up to 34% genomic editing yielding 80% FIS-responsive organoids; Isc rescue in HNE cells	GUIDE-seq and deep sequencing detected no editing at predicted off-target loci	Anzalone et al. (2019); Bulcaen et al. (2024)

Table 4. Artificial intelligence and computer vision frameworks for high-throughput organoid image analytics. Six analytical pipelines are compared by neural network architecture, accepted image type and plate format, the features each extracts, reported accuracy, application in cystic fibrosis research, and availability. Because these tools extract different quantities — bounding-box area, segmented boundary, luminal fraction, or frame-to-frame difference — they are not directly interchangeable, and swelling distributions derived from one pipeline should not be pooled with those from another without cross-validation. All six are open source.

Framework	Neural network architecture	Input image type and format	Analytical functions and features extracted	Reported accuracy metrics	Application in CF research	Availability	Key references
OrgaQuant	Deep convolutional neural network, end-to-end object detector	Label-free brightfield live-cell images; 96- and 384-well plates	Organoid localization via bounding boxes; particle tracking over time; per-organoid swell rate	Swell rates match fluorescent AUC (R^2 = 0.91)	Automated label-free FIS screening of FDA drug libraries in 384-well nasal organoids	Open-source (GitHub)	Kassis et al. (2019); de Poel et al. (2022)
DETECTOR	Dual model: VGG19 Gaussian density map plus YOLOv7-E6E object detector	Dynamic brightfield time-lapse series (120 min); 96-well format	Density-map organoid counting; frame differencing (t vs. t) classifying swelling organoids	Counting accuracy 94% (MAE 5.20%); swelling detection AP = 0.85	Dynamic label-free quantification of functional CFTR rescue after prime editing	Open-source (Dataverse)	Bulcaen et al. (2024)
OrgaSegment	Deep-learning semantic segmentation network	Brightfield and confocal live-cell imaging; 96/384-well microplates	Precise lumen and total surface boundary segmentation; fluid secretion tracking	High-precision boundary segmentation overcoming Matrigel optical distortion	High-content quantification of CFTR-dependent lumen expansion and SLA metrics	Open-source (GitHub)	Lefferts et al. (2024)
OrganoSeg	Threshold-based automated morphometry software	Brightfield live-cell images of 3D organoid populations	Binarization, area extraction, organoid count and cross-sectional area	Automated whole-well CSA segmentation; requires manual filtering of edge objects	Automated image processing for iPSC-derived airway spheroid FIS quantification	Open-source (MATLAB)	Borten et al. (2018); Berical et al. (2022)
Cellpose / Cellpose-SAM	Deep-learning cellular segmentation integrated with Segment Anything Model	Multi-channel fluorescent and brightfield 3D organoid z-stacks	Cellular and sub-organoid segmentation; nuclear and lumen tracking	Zero-shot generalization across diverse organoid morphologies	Multi-parametric single-cell and organoid feature extraction in HTS screening	Open-source (Python)	Pachitariu et al. (2025); Boonekamp & Boutros (2026)
HCS-3DX / digitalized organoids	Multilevel AI segmentation with digital marker derivation algorithms	High-content 3D confocal volumetric imaging in 384-well plates	3D structural reconstruction, cellular topology, viability and phenotypic state clustering	High-speed 3D structural analysis across thousands of objects per well	Cross-modal integration of organoid phenotypic profiling with transcriptomic data	Open-source	Diosdi et al. (2025); Ong et al. (2025)

applied to identical image sets will not return identical swelling distributions, and cross-tool validation remains sparse.

4.3 Resolving geometrical barriers: functional interrogation of apical ion channels

Removing the extracellular matrix allows intestinal and iPSC-derived organoids to split open into planar monolayers with an upward-facing apical membrane (Xia et al., 2021). Quantitative PCR and immunofluorescence confirm that these preparations preserve tight junction integrity (ZO-1) and maintain CFTR, ENaC, and SLC6A14 expression at levels comparable to intact 3D structures — the necessary precondition for treating the opened preparation as physiologically equivalent (Xia et al., 2021; Xia, 2022). Figure 3 summarizes the transformation and the three assays it supports.

Coupled to the FLIPR Tetra platform, opened organoids permit kinetic interrogation of multiple apical transport systems (Ahmadi et al., 2017; Xia et al., 2021):

• Apical chloride conductance (ACC). In zero-sodium/chloride buffer, forskolin stimulation drives CFTR-mediated anion efflux and consequent membrane depolarization, registered as increased FLIPR fluorescence. Wild-type opened organoids gave an EC of 0.0287 µM for forskolin with a Z factor of 0.5294, confirming HTS compatibility. In F508del preparations, chronic elexacaftor/tezacaftor rescue followed by acute ivacaftor produced marked depolarization, which co-treatment with phosphodiesterase inhibitors such as milrinone further enhanced (Xia et al., 2021).

• Apical sodium conductance (ASC). In physiological sodium buffer, apical amiloride or phenamil at 10–50 µM evoked rapid hyperpolarization. The assay returned a Z of 0.573, establishing the first HTS-compatible route to ENaC inhibitor screening in patient-derived human epithelia (Xia et al., 2021).

• Apical amino acid conductance (AAC). Under low sodium/chloride gradients, apical L-arginine at 1 mM induced electrogenic uptake through SLC6A14 and net depolarization; pre-treatment with the selective blocker -methyl-DL-tryptophan at 2 mM abolished the response entirely, confirming transporter specificity (Xia et al., 2021).

The trade-off is explicit and should be stated: opening the organoid gains apical access at the cost of the volumetric swelling readout, so ACC/ASC/AAC assays complement FIS rather than replacing it (Table 2).

4.4 Functional validation of RNA modulators and high-fidelity gene editing

Organoid HTS has become the default validation layer for therapies targeting drug-refractory PTCs — W1282X, G542X, S308X — and complex missense variants (Table 3; Figure 4) (Geurts et al., 2020; Bulcaen et al., 2024). High-content 384-well platforms employing lipid nanoparticle or electroporation delivery support rapid screening of ASOs, siRNAs, and shRNAs (del Angel Zuvirie et al., 2022). For deep intronic splicing mutations such as 3849+10 kb C>T, splice-switching ASOs restore full-length CFTR mRNA and functional swelling (Oren et al., 2021).

Across editing modalities, the pattern is one of successive risk reduction. CRISPR/Cas9 HDR correction of F508del in intestinal stem cell organoids restored FIS to 167–187% of wild-type controls, an effect fully blocked by CFTRinh-172 and therefore attributable to CFTR (Schwank et al., 2013). Adenine base editing avoided double-strand breaks altogether, achieving A·T G·C transitions that convert TAG stop codons to TGG in primary rectal organoids carrying W1282X and R553X, with full restoration of protein synthesis and swelling (Geurts et al., 2020). Prime editing extended the reach further: PE3 and PE5max constructs delivered lentivirally into primary rectal organoids and ALI-differentiated human nasal epithelial cells corrected L227R and N1303K with genomic repair efficiencies up to 34%, yielding up to 80% functionally rescued, swelling-competent organoids, with GUIDE-seq and deep sequencing detecting no off-target editing at predicted loci (Anzalone et al., 2019; Bulcaen et al., 2024).

Two caveats temper this. Percentage restoration relative to wild-type is a ratio whose denominator varies with assay conditions, so figures above 100% indicate assay-specific scaling rather than supraphysiological function. And absence of detected off-target editing at predicted loci is not equivalent to absence of off-target editing, a distinction that matters considerably more for a therapy than for a proof of concept.

5. What Organoid Screening Has Established, and What It Has Not

5.1 The validity case is strong, but it is a validity of function rather than of tissue

The most consistent finding across this literature is that patient-derived organoids report CFTR function accurately enough to guide clinical decisions. That conclusion rests on a specific and reasonably robust chain of evidence: FIS is pharmacologically CFTR-dependent (Dekkers et al., 2013); baseline swelling tracks residual channel activity across genotypes (Berkers et al., 2019); post-rescue swelling correlates with sweat chloride and ppFEV in independent cohorts (Dekkers et al., 2016; de Winter-de Groot et al., 2019); and the ranking of modulator combinations in organoids matches their ranking in trials (Keating et al., 2018; Berkers et al., 2019) (Table 2; Figure 1).

It is worth being precise about what this does and does not establish. The validity demonstrated is functional, not anatomical. A rectal organoid is not a lung, and its predictive value derives from the fact that CFTR behaves similarly in both epithelia under cAMP stimulation, not from any structural resemblance. This matters because it bounds the inferences one may draw. Organoid FIS can indicate whether a given patient's CFTR responds to a given compound; it cannot indicate how that response will interact with airway inflammation, mucus rheology, established bronchiectasis, or infection burden. Correlations of r 0.6–0.7 with ppFEV are strong for a preclinical assay yet leave roughly half the variance in lung function unexplained — which is exactly what one should expect, since lung function in CF is determined by much more than channel activity. Presenting organoid response as a predictor of clinical outcome, rather than as a predictor of CFTR rescue, overstates the case.

The tissue-specificity gap is therefore real but frequently misdescribed. Intestinal organoids lack respiratory features — ENaC expression patterns, mucociliary transport, lung-specific modifiers (Table 1) — and no amount of protocol refinement will supply them. The productive response has not been to abandon intestinal models but to pair them with airway systems. NAOs conditioned with interleukin-1 and neuregulin-1 achieved close alignment with matched intestinal AUC (r = 0.9689), which suggests the two are measuring a shared quantity when the airway model is appropriately matured (Amatngalim et al., 2022). iPSC-derived airway organoids offer isogenic comparison and unlimited expansion at the cost of protracted differentiation and variable maturation state (Berical et al., 2022; McCauley et al., 2018; Tsai et al., 2025). Neither displaces the other.

5.2 Scalability has been solved in engineering terms; reproducibility has not

Miniaturization, robotic handling, and deep-learning analysis have collectively removed the throughput ceiling (Figure 2; Table 4). Z factors above 0.5 and coefficients of variation below roughly 12% under standardized protocols place the assay comfortably within accepted HTS parameters (Vonk et al., 2020; de Poel et al., 2022). On any reasonable engineering criterion, the scaling problem is solved.

Reproducibility is a different matter, and it is here that the field's confidence should be more measured. Bierlaagh et al. (2024) examined repeatability and reproducibility of FIS directly and found variability that standardized protocols reduce but do not eliminate — an honest and necessary contribution in a literature that otherwise tends to report best-case performance. Matrigel remains an animal-derived, lot-variable substrate, and defined synthetic hydrogels are proposed rather than established. Organoid size heterogeneity and baseline swelling variation persist as noise sources even under calibrated forskolin concentrations.

A subtler issue attaches to the analytical tools themselves. OrgaQuant, DETECTOR, OrgaSegment, OrganoSeg, and generalist segmentation models differ in architecture, training data, and the quantity they actually extract — bounding-box area, segmented boundary, luminal fraction, frame difference (Table 4) (Kassis et al., 2019; Borten et al., 2018; Bulcaen et al., 2024; Lefferts et al., 2024; Pachitariu et al., 2025). These are not interchangeable measurements. Applied to the same images, they will not return identical swelling distributions, and published cross-tool comparisons remain scarce. As automated analysis becomes standard, the choice of pipeline becomes a source of between-laboratory variance that is currently under-reported. Open-source availability helps, but availability is not the same as harmonization.

5.3 Apical access opens genotype-agnostic targets, on a narrower evidence baseThe opened-organoid platform is conceptually the most

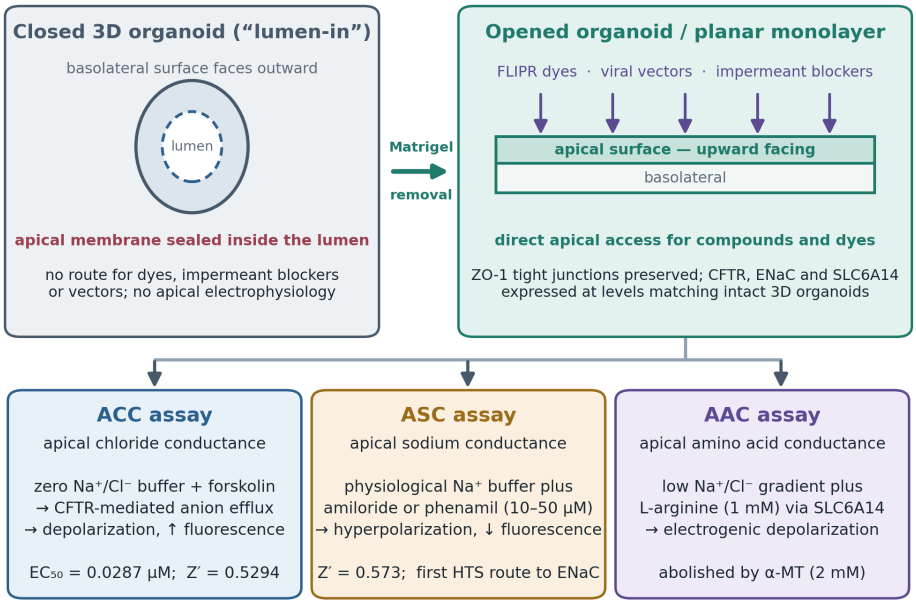

Figure 3. Opened-organoid preparations resolve the apical access barrier and extend screening to companion ion transport targets. In the intact spherical organoid (left), the apical membrane — where CFTR, ENaC, TMEM16A, and SLC6A14 reside — is sealed within an internal lumen, excluding impermeant compounds, viral vectors, and membrane potential dyes and precluding apical electrophysiology. Removing extracellular matrix support allows the sphere to split mechanically into a planar monolayer presenting the apical surface upward (right), while preserving ZO-1 tight junction integrity and maintaining CFTR, ENaC, and SLC6A14 expression at intact-3D levels. Three FLIPR-based assays follow directly from this geometry, each with its reported performance statistics. The trade-off is that the volumetric swelling readout is lost, so these assays complement rather than replace FIS. Constructed from Ahmadi et al. (2017), Xia et al. (2021), and Xia (2022).

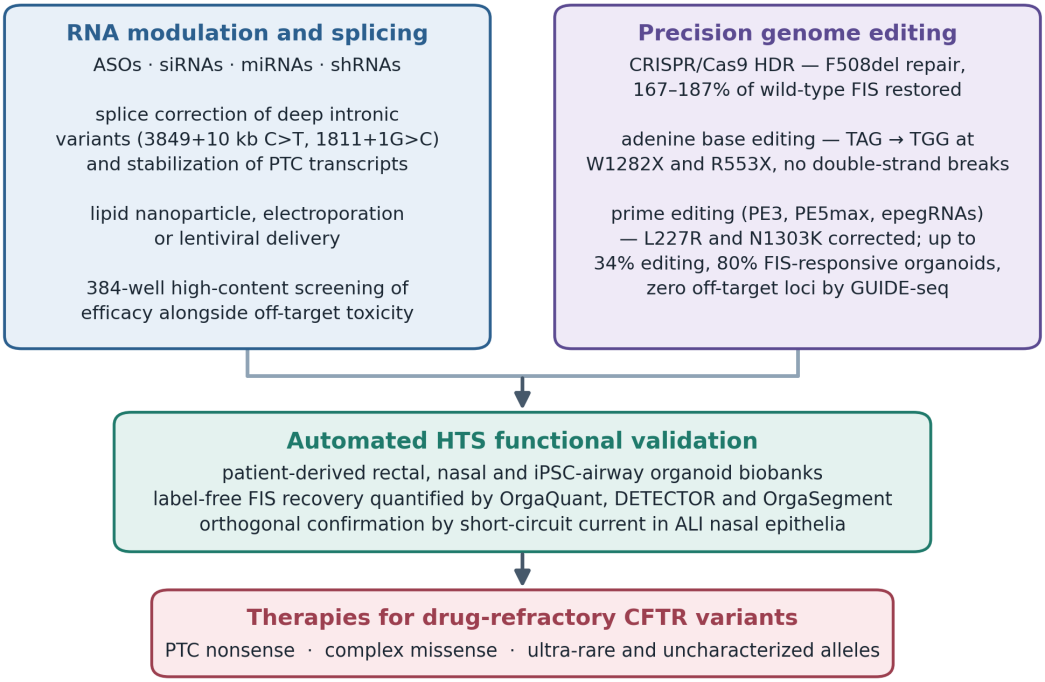

Figure 4. Convergence of RNA modulation and precision genome editing on a shared automated functional readout. Two therapeutic streams address the drug-refractory genotypes that small-molecule modulators cannot reach. RNA-based approaches (left) correct aberrant splicing or stabilize transcripts and are screened at 384-well scale for efficacy alongside off-target cytotoxicity. Genome editing approaches (right) repair the endogenous locus directly, progressing from CRISPR/Cas9 homology-directed repair through adenine base editing to prime editing, a sequence that represents successive reduction in double-strand-break-associated risk. Both streams converge on automated high-throughput functional validation in patient-derived organoid biobanks, with orthogonal confirmation by short-circuit current in air–liquid interface nasal epithelia. Constructed from Schwank et al. (2013), Anzalone et al. (2019), Geurts et al. (2020), Oren et al. (2021), del Angel Zuvirie et al. (2022), and Bulcaen et al. (2024).

significant methodological advance reviewed here, because it removes a constraint that was architectural rather than incidental (Figure 3). Access to the apical membrane makes ENaC, TMEM16A, and SLC6A14 screenable in patient-derived human tissue for the first time, and each of these is genotype-agnostic — relevant, in principle, to every patient including those with no translated CFTR protein at all (Xia et al., 2021; Pacheco et al., 2022). For the 10% whom modulators cannot help, that is the difference between a target and no target.

The evidence base, however, is considerably thinner than for FIS. The ACC, ASC, and AAC assays derive principally from a single research programme (Ahmadi et al., 2017; Xia et al., 2021; Xia, 2022), and the key validation report remains a preprint. Reported Z values of 0.5294 and 0.573 sit only modestly above the conventional 0.5 threshold, leaving limited margin for the additional variance that multi-site deployment invariably introduces. Independent replication in other laboratories, and in airway-derived rather than intestinal material, is the obvious prerequisite before these assays can carry the weight currently placed on them. None of this diminishes the concept; it simply locates it earlier on the maturity curve than the FIS literature.

5.4 Gene editing validation exposes the limits of a functional readout

Organoids have become the standard proving ground for successive editing generations, and the trajectory from CRISPR/Cas9 HDR through base editing to prime editing represents a genuine reduction in genotoxic risk (Table 3; Figure 4) (Schwank et al., 2013; Geurts et al., 2020; Anzalone et al., 2019; Bulcaen et al., 2024). Prime editing correcting L227R and N1303K — variants for which no modulator works — at up to 34% efficiency with 80% of organoids rendered swelling-competent is a substantial result (Bulcaen et al., 2024).

Two interpretive cautions apply. First, a functional swelling readout confirms that CFTR works; it says nothing about how the edit was achieved or what else changed. Restoration figures expressed as a percentage of wild-type are ratios sensitive to assay scaling, and values exceeding 100% reflect that scaling rather than supraphysiological channel activity. Second, and more consequentially, off-target profiling by GUIDE-seq and targeted deep sequencing interrogates predicted loci. Absence of detected editing at predicted sites is weaker evidence than it appears, and the gap between it and genuine genome-wide safety is the gap that must be closed before clinical translation. Organoids are well suited to demonstrating efficacy and poorly suited to excluding rare genotoxic events, since the latter requires sequencing depth and cell numbers that organoid culture does not readily provide.

There is also the delivery problem, which organoid work largely brackets. Lentiviral and electroporation-based delivery used in these studies is appropriate for ex vivo proof of concept but is not the route by which an editing therapy would reach an airway in vivo. Demonstrating correction in an organoid establishes that the edit is possible and productive; it leaves the harder translational question untouched.

5.5 Implications for personalized medicine and regulatory pathways

The clearest clinical contribution of organoid theratyping is to patients whom genotype-based prescribing cannot serve. HIT-CF and comparable programmes have converted organoid response into actual access decisions — off-label approval, compassionate use, trial enrichment — for individuals whose variants are too rare to support a conventional trial (van Mourik et al., 2020; Ramalho et al., 2021). For an ultra-rare allele, an n-of-1 functional test may be the only evidence that will ever exist, and refusing to act on it is itself a decision with consequences.

Two obstacles stand between current practice and routine adoption. The first is regulatory: no framework presently qualifies organoid response as a surrogate endpoint, so its use remains discretionary and jurisdictionally uneven (Conti et al., 2022). Qualification will require prospectively defined thresholds, standardized protocols, and demonstrated inter-laboratory reproducibility — which returns the argument to Section 5.2, and makes reproducibility work a regulatory prerequisite rather than a methodological nicety. The second is ethical and practical. Fawcett et al. (2021) found the Australian CF community broadly receptive to personalized organoid technology while raising concerns about expectation management, consent, and equitable access. Those concerns are well founded. A platform that depends on biopsy, specialist biobanking infrastructure, and expensive recombinant growth factors will not distribute evenly, and the patients with the rarest variants are not necessarily those with the best access to tertiary centres.

5.6 Limitations of this study

Several constraints bound what can be concluded here. The review is narrative rather than systematic, so findings were weighted by judgement rather than by predefined rules, and no meta-analysis was attempted. Publication bias toward successful assay development is likely substantial in a field where methodological tool papers are the dominant output; unsuccessful screens and non-reproducible assays are rarely published. A number of quantitative values reported throughout — EC and Z figures for the opened-organoid assays in particular — derive from single studies or single laboratories and await independent confirmation. Finally, the corpus is weighted toward intestinal and rectal models simply because they are older and more widely adopted, which may understate both the current maturity and the residual limitations of airway-derived systems.

6. Conclusion

High-throughput organoid screening has moved from a promising assay to working translational infrastructure for cystic fibrosis. The functional validity of forskolin-induced swelling is well supported: it is CFTR-dependent, tracks residual channel activity, and correlates with sweat chloride and ppFEV closely enough to have guided real prescribing decisions for patients with rare variants. Miniaturization into 384-well formats and deep-learning image analysis have removed the throughput ceiling, while opened-organoid preparations have extended screening to ENaC, TMEM16A, and SLC6A14 — targets relevant even to patients who make no CFTR protein at all. What remains unfinished is less biological than institutional. Inter-laboratory reproducibility, harmonization of analytical pipelines, replacement of animal-derived matrix, and a regulatory framework qualifying organoid response as a surrogate endpoint are the conditions on which routine clinical adoption depends. These are tractable problems, and none of them requires a conceptual breakthrough.

References

Ahmadi, S., Xia, S., Wu, Y. S., Di Paola, M., Laselva, O., Avolio, J., & Bear, C. E. (2017). Phenotypic profiling of CFTR modulators in patient-derived respiratory epithelia. npj Genomic Medicine, 2(1), 12.

Amatngalim, G. D., Rodenburg, L. W., Aalbers, B. L., Raeven, H. H., Aarts, E. M., Sarhane, D., Spelier, S., Lefferts, J. W., Silva, I. A. L., & Nijenhuis, W. (2022). Measuring cystic fibrosis drug responses in organoids derived from 2D differentiated nasal epithelia. Life Science Alliance, 5(12), e202101320.

Amistadi, S., Maule, G., Ciciani, M., Ensinck, M. M., De Keersmaecker, L., Ramalho, A. S., Guidone, D., Buccirossi, M., Galietta, L. J. V., Carlon, M. S., & Cereseto, A. (2023). Functional restoration of a CFTR splicing mutation through RNA delivery of CRISPR adenine base editor. Molecular Therapy, 31(5), 1647–1660.

Anzalone, A. V., Randolph, P. B., Davis, J. R., Sousa, A. A., Koblan, L. W., Levy, J. M., Chen, P. J., Wilson, C., Newby, G. A., Raguram, A., & Liu, D. R. (2019). Search-and-replace genome editing without double-strand breaks or donor DNA. Nature, 576(7785), 149–157.

Berical, A., Lee, R. E., Lu, J., Beermann, M. L., Le Suer, J. A., Mithal, A., Thomas, D., Ranallo, N., Peasley, M., Stuffer, A., & Hawkins, F. (2022). A multimodal iPSC platform for cystic fibrosis drug testing. Nature Communications, 13(1), 4270.

Berkers, G., van Mourik, P., Vonk, A. M., Kruisselbrink, E., Dekkers, J. F., de Winter-de Groot, K. M., Arets, H. G. M., Marck-van der Wilt, R. E. P., Dijkema, J. S., Vanderschuren, M. M., & Beekman, J. M. (2019). Rectal organoids enable personalized treatment of cystic fibrosis. Cell Reports, 26(7), 1701–1708.

Bierlaagh, M. C., Ramalho, A. S., Silva, I. A., Vonk, A. M., van den Bor, R. M., van Mourik, P., Pott, J., Suen, S. W. F., Boj, S. F., Vries, R. G. J., & Beekman, J. M. (2024). Repeatability and reproducibility of the forskolin-induced swelling (FIS) assay on intestinal organoids from people with cystic fibrosis. Journal of Cystic Fibrosis, 23(4), 693–702.

Boj, S. F., Vonk, A. M., Statia, M., Su, J., Vries, R. R. G., Beekman, J. M., & Clevers, H. (2017). Forskolin-induced swelling in intestinal organoids: An in vitro assay for assessing drug response in cystic fibrosis patients. Journal of Visualized Experiments, (120), e55159.

Boonekamp, K. E., & Boutros, M. (2026). Primer: Drug discovery and patient-derived organoids. Current Opinion in Systems Biology, 45, 100579.

Borten, M. A., Bajikar, S. S., Sasaki, N., Clevers, H., & Janes, K. A. (2018). Automated brightfield morphometry of 3D organoid populations by OrganoSeg. Scientific Reports, 8(1), 5319.

Brewington, J. J., Filbrandt, E. T., LaRosa, F. J., Ostmann, A. J., Strecker, L. M., Szczesniak, R. D., & Clancy, J. P. (2018). Detection of CFTR function and modulation in primary human nasal cell spheroids. Journal of Cystic Fibrosis, 17(1), 26–33.

Bulcaen, M., Kortleven, P., Liu, R. B., Maule, G., Dreano, E., Kelly, M., Ensinck, M. M., Thierie, S., Smits, M., Ciciani, M., Hatton, A., Chevalier, B., & Carlon, M. S. (2024). Prime editing functionally corrects cystic fibrosis-causing CFTR mutations in human organoids and airway epithelial cells. Cell Reports Medicine, 5(5), 101544.

Conti, J., Sorio, C., & Melotti, P. (2022). Organoid technology and its role for theratyping applications in cystic fibrosis. Children, 10(1), 4.

Cutting, G. R. (2015). Cystic fibrosis genetics: From molecular understanding to clinical application. Nature Reviews Genetics, 16(1), 45–56.

de Poel, E., Spelier, S., Hagemeijer, M. C., & Beekman, J. M. (2023). FDA-approved drug screening in patient-derived organoids demonstrates potential of drug repurposing for rare

cystic fibrosis genotypes. Journal of Cystic Fibrosis, 22(3), 548–559.

de Poel, E., Spelier, S., Hagemeijer, M. C., van der Windt, I. S., van Hugten, C. F. J., van Beuningen, S. F. B., Rodenburg, R. N. P., & Beekman, J. M. (2022). Drug repurposing for cystic fibrosis: Identification of drugs that induce CFTR-independent fluid secretion in nasal organoids. International Journal of Molecular Sciences, 23(20), 12657.

de Winter-de Groot, K. M., Berkers, G., Marck-van der Wilt, R. E. P., van der Meer, R., Vonk, A., Dekkers, J. F., Geerdink, M., Michel, S., Kruisselbrink, E., Vries, R., & Beekman, J. M. (2019). Forskolin-induced swelling of intestinal organoids correlates with disease severity in adults with cystic fibrosis and homozygous F508del mutations. Journal of Cystic Fibrosis, 18(5), 614–619.

Dekkers, J. F., Berkers, G., Kruisselbrink, E., Vonk, A., de Jonge, H. R., Janssens, H. M., Bronsveld, I., van de Graaf, E. A., Nieuwenhuis, E. E. S., Houwen, R. H. J., & Beekman, J. M. (2016). Characterizing responses to CFTR-modulating drugs using rectal organoids derived from subjects with cystic fibrosis. Science Translational Medicine, 8(344), 344ra84.

Dekkers, J. F., Wiegerinck, C. L., de Jonge, H. R., Bronsveld, I., Janssens, H. M., de Winter-de Groot, K. M., Brandsma, A. M., de Jong, N. W. M., Bijvelds, M. J. C., Scholte, B. J., & Beekman, J. M. (2013). A functional CFTR assay using primary cystic fibrosis intestinal organoids. Nature Medicine, 19(7), 939–945.

del Angel Zuvirie, C., van der Drift, L., Yan, K., Price, L. S., & Bange, H. (2022). Enabling RNA-based gene modification in high-throughput screenings using cystic fibrosis patient-derived organoids. Journal of Cystic Fibrosis, 21(Suppl. 1), S103–S104.

Demchenko, A., Balyasin, M., Nazarova, A., Grigorieva, O., Panchuk, I., Kondrateva, E., Tabakov, V., Schagina, O., Amelina, E., & Smirnikhina, S. (2025). Human induced lung organoids: A promising tool for cystic fibrosis drug screening. International Journal of Molecular Sciences, 26(1), 437.

Diosdi, A., Toth, T., Harmati, M., Istvan, G., Schrettner, B., Hapek, N., Kovacs, F., Kriston, A., Buzas, K., Pampaloni, F., Piccinini, F., & Horvath, P. (2025). HCS-3DX, a next-generation AI-driven automated 3D-oid high-content screening system. Nature Communications, 16(1), 8897.

Fawcett, L. K., Wakefield, C. E., Sivam, S., Middleton, P. G., Wark, P., Widger, J., Jaffe, A., & Waters, S. A. (2021). Avatar acceptability: Views from the Australian cystic fibrosis community on the use of personalised organoid technology to guide treatment decisions. ERJ Open Research, 7(1), 00448-2020.

Geurts, M. H., de Poel, E., Amatngalim, G. D., Oka, R., Meijers, F. M., Kruisselbrink, E., van Mourik, P., Berkers, G., de Winter-de Groot, K. M., Michel, S., & Clevers, H. (2020). CRISPR-based adenine base editing corrects cystic fibrosis mutations in intestinal organoids. Cell Stem Cell, 26(4), 503–510.

Guimbellot, J. S., Leach, J. M., Chaudhry, I. G., Quinney, N. L., Boyles, S. E., Chua, M., Aban, I., Jaspers, I., & Gentzsch, M. (2017). Nasospheroids permit measurements of CFTR-dependent fluid transport. JCI Insight, 2(21), e95734.

Hagemeijer, M. C., Vonk, A. M., Awatade, N. T., Silva, I. A., Tischer, C., Hilsenstein, V., Beekman, J. M., Amaral, M. D., & Botelho, H. M. (2020). An open-source high-content analysis workflow for CFTR function measurements using the forskolin-induced swelling assay. Bioinformatics, 36(24), 5686–5694.

Kassis, T., Hernandez-Gordillo, V., Langer, R., & Griffith, L. G. (2019). OrgaQuant: Human intestinal organoid localization and quantification using deep convolutional neural networks. Scientific Reports, 9(1), 12479.

Keating, D., Marigowda, G., Burr, L., Daines, C., Mall, M. A., McKone, E. F., Ramsey, B. W., Rowe, S. M., Taylor-Cousar, J. L., & Waltz, D. (2018). VX-445–tezacaftor–ivacaftor in patients with cystic fibrosis and one or two Phe508del alleles. New England Journal of Medicine, 379(17), 1612–1620.

Lefferts, J. W., Kroes, S., Smith, M. B., Niemöller, P. J., Nieuwenhuijze, N. D., Sonneveld van Kooten, H. N., van der Ent, C. K., Beekman, J. M., & van Beuningen, S. F. (2024). OrgaSegment: Deep-learning based organoid segmentation to quantify CFTR dependent fluid secretion. Communications Biology, 7(1), 319.

Lim, S. H., Aboualizadeh, F., Petschnigg, J., & Stagljar, I. (2021). Identification of FGL2 as a novel regulator of CFTR maturation and function using primary intestinal organoids. Molecular Systems Biology, 17(11), e10629.

Martin, U. (2015). Pluripotent stem cells for disease modeling and drug screening: New perspectives for treatment of cystic fibrosis? Molecular and Cellular Therapies, 3(1), 1–12.

McCauley, K. B., Hawkins, F., Serra, M., Thomas, D. C., Jacob, A., & Kotton, D. N. (2018). Efficient derivation of functional human airway epithelium from pluripotent stem cells via temporal regulation of Wnt signaling. Cell Stem Cell, 20(6), 844–857.

Ong, H. T., Karatas, E., Poquillon, T., Grenci, G., Furlan, A., Dilasser, F., & Virzì, A. (2025). Digitalized organoids: Integrated pipeline for high-speed 3D analysis of organoid structures using multilevel segmentation and cellular topology. Nature Methods, 22(7), 1343–1354.

Oren, Y. S., Irony-Tur Sinai, M., Golec, A., Barchad-Avitzur, O., Mutyam, V., Li, Y., Hong, J., Ozeri-Galai, E., Hatton, A., Leibson, C., & Kerem, E. (2021). Antisense oligonucleotide-based drug development for cystic fibrosis patients carrying the 3849+10 kb C-to-T splicing mutation. Journal of Cystic Fibrosis, 20(5), 865–875.

Pacheco, M. L., Silva, I. A. L., Railean, V., & Amaral, M. D. (2022). Novel cell models for cystic fibrosis drug development and personalized medicine. Journal of Personalized Medicine, 12(8), 1321.

Pachitariu, M., Rariden, M., & Stringer, C. (2025). Cellpose-SAM: Superhuman generalization for cellular segmentation. bioRxiv.

Pranke, I. M., Hatton, A., Simonin, J., Jais, J. P., Le Pimpec-Barthes, F., Carsin, A., Bonnette, P., Fayon, M., Stremler-Le Bel, N., Grenet, D., & Sermet-Gaudelus, I. (2017). Correction of CFTR function in nasal epithelial cells from cystic fibrosis patients predicts improvement of respiratory function by CFTR modulators. Scientific Reports, 7(1), 7375.

Ramalho, A. S., Furstova, E., Vonk, A. M., Ferrante, M., Verfaillie, C., Dupont, L., Boon, M., Proesmans, M., Beekman, J. M., Sarouk, I., & De Boeck, K. (2021). Correction of CFTR function in intestinal organoids to guide treatment of cystic fibrosis. European Respiratory Journal, 57(1), 1902426.

Ratjen, F., Bell, S. C., Rowe, S. M., Goss, C. H., Quittner, A. L., & Bush, A. (2015). Cystic fibrosis. Nature Reviews Disease Primers, 1, 15010.

Sato, T., Vries, R. G., Snippert, H. J., van de Wetering, M., Barker, N., Stange, D. E., van Es, J. H., Abo, A., Kujala, P., Peters, P. J., & Clevers, H. (2009). Single Lgr5 stem cells build crypt-villus structures in vitro without a mesenchymal niche. Nature, 459(7244), 262–265.

Schwank, G., Koo, B. K., Sasselli, V., Dekkers, J. F., Heo, I., Demircan, T., Steiner, N., Lawrence, A. C., & Clevers, H. (2013). Functional repair of CFTR by CRISPR/Cas9 in intestinal stem cell organoids of cystic fibrosis patients. Cell Stem Cell, 13(6), 653–658.

Tsai, P. H., Yang, Y. P., Wang, C. H., Liang, K. H., Yeh, C. L., Huang, T. Y., Hwang, T. C., Lo, W. L., Lan, Y. T., Ching, L. J., Wang, M. L., Huo, T. L., Luo, Y. H., Chiou, S. H., & Chou, S. J. (2025). Multimodal single-cell transcriptomics with patient-specific iPSC-derived airway organoids as a drug screening approach for cystic fibrosis with nonsense mutations. Biomedicine & Pharmacotherapy, 191, 118476.

Vaidyanathan, S., Salahudeen, A. A., Sellers, Z. M., Bravo, D. T., Choi, S. S., Batish, A., Le, W., Baik, R., de la O, S., Kaushik, M. P., & Porteus, M. H. (2020). High-efficiency, selection-free gene repair in airway stem cells from cystic fibrosis patients rescues CFTR function in differentiated epithelia. Cell Stem Cell, 26(2), 161–171.

van Mourik, P., Beekman, J. M., & van der Ent, C. K. (2019). Intestinal organoids to model cystic fibrosis. European Respiratory Journal, 54(1), 1802379.

van Mourik, P., Michel, S., Vonk, A. M., Beekman, J. M., & van der Ent, C. K. (2020). Rationale and design of the HIT-CF organoid study: Stratifying cystic fibrosis patients based on intestinal organoid response to different CFTR-modulators. BMC Pulmonary Medicine, 20(1), 60.

Vonk, A. M., van Mourik, P., Ramalho, A. S., Silva, I. A. L., Statia, M., Kruisselbrink, E., Suen, S. W. F., Dekkers, J. F., Vleggaar, F. P., Houwen, R. H. J., & Beekman, J. M. (2020). Protocol for application, standardization and validation of the forskolin-induced swelling assay in cystic fibrosis human colon organoids. STAR Protocols, 1(1), 100019.

Xia, S. (2022). High-throughput screening assays for novel cystic fibrosis therapies [Doctoral dissertation, University of Toronto]. University of Toronto Research Repository.

Xia, S., Bozóky, Z., Laselva, O., Di Paola, M., Ahmadi, S., Jiang, J. X., ... & Bear, C. E. (2021). High-throughput functional analysis of CFTR and other apically localized channels in iPSC derived intestinal organoids. bioRxiv, 2021-07.